

Method for Preparing Carbon Supported Pt–Ru Nanoparticles with Controlled Internal Structure

Tapan K. Sau,^{†,§} Marco Lopez,[‡] and Dan V. Goia^{*,†}[†]Center for Advanced Materials Processing (CAMP), Clarkson University, P.O. Box 5814, Potsdam, New York 13699-5814, and [‡]Rodenbacher Chaussee 4, 63403, Hanau, Germany. [§]Present Address: Department of Physics and Center for Nanoscience, Ludwig-Maximilians-Universitaet Muenchen, Amalienstr. 54, D-80799 Munich, Germany.

Received April 17, 2009. Revised Manuscript Received June 19, 2009

A polyol method for depositing highly dispersed PtRu nanoparticles with controlled size and internal composition on carbon supports is described. Through a judicious selection of the polyol, reaction pH and temperature, and modality of combining the reactants, it was possible to control not only the size and dispersion of the bimetallic nanoparticles but also the relative spatial distribution of the two elements. The method yields reproducibly high metal-loading electrocatalysts in which the Pt:Ru ratio in both the surface and the interior of the particles can be tailored. The strategy described represents a viable experimental approach for controlling the internal composition of other bi- or multimetallic systems.

Introduction

The increasing demand for fuel cells as stationary and portable power sources has been a major reason for the recent resurgence of research in the field of nanocatalysis.^{1–3} It was amply demonstrated that carbon supported Pt nanoparticles are very effective electrocatalysts for PEM fuel cells.^{4–13} Pure platinum electrodes, however, are sensitive to CO poisoning, a phenomenon which drastically affects cell performance.^{14–17} This has led to the development of Pt-based binary, ternary, and quaternary metallic systems including cocatalysts such as Ru,

Sn, Fe, W, Mo, and so forth.^{15,17–26} To date, the Pt–Ru binary system appears to be the most CO-tolerant catalyst for hydrogen and/or methanol electro-oxidation.^{14,15,22,27} It has also been demonstrated that “alloyed” PtRu nanoparticles have an improved chemical stability.²⁸ Because of the important role of the relative “spatial” distribution of the two elements, there is still a great deal of interest in synthesizing PtRu nanoparticles with variable degrees of components intermixing.^{16,17,23,29–32}

Coprecipitation,^{11,33,34} coimpregnation,^{28,35} colloid adsorption,³⁶ and surface organometallic chemistry⁴ are

- (1) Gates, B. C.; Gucci, L.; Knoezinger, H. *Metal Clusters in Catalysis*; Elsevier: Amsterdam, 1986.
- (2) Sinfelt, J. H. *Bimetallic Catalysts - Discoveries, Concepts, and Applications*; Wiley: New York, 1983.
- (3) Toshima, N.; Yonezawa, T. *New J. Chem.* **1998**, 1179.
- (4) King, W. D.; Corn, J. D.; Murphy, O. J.; Boxall, D. L.; Kenik, E. A.; Kwiatkowski, K. C.; Stock, S. R.; Lukehart, C. M. *J. Phys. Chem. B* **2003**, 107, 5467.
- (5) Venkataraman, R.; Kunz, H. R.; Fenton, J. M. *J. Electrochem. Soc.* **2003**, 150, A278.
- (6) Ralph, T. R.; Hogarth, M. P. *Platinum Met. Rev.* **2002**, 46, 117.
- (7) Boxall, D. L.; Deluga, G. A.; Kenik, E. A.; King, W. D.; Lukehart, C. M. *Chem. Mater.* **2001**, 13, 891.
- (8) Waszczuk, P.; Solla-Gullón, J.; Kim, H. S.; Tong, Y. Y.; Montiel, V.; Aldaz, A.; Wieckowski, A. *J. Catal.* **2001**, 203, 1.
- (9) Long, J. W.; Stroud, R. M.; Swider-Lyons, K. E.; Rolison, D. R. *J. Phys. Chem. B* **2000**, 104, 9772.
- (10) Bönnemann, H.; Brinkmann, R.; Britz, P.; Endruschat, U.; Mörtel, R.; Paulus, U. A.; Feldmeyer, G. J.; Schmidt, T. J.; Gasteiger, H. A.; Behm, R. J. *New Mater. Electrochem. Syst.* **2000**, 3, 199.
- (11) Gurau, B.; Viswanathan, R.; Liu, R.; Lafrenz, T. J.; Ley, K. L.; Smotkin, E. S.; Reddington, E.; Sapienza, A.; Chan, B. C.; Mallouk, T. E.; Sarangapani, S. *J. Phys. Chem. B* **1998**, 102, 9997.
- (12) Nashner, M. S.; Frenkel, A. I.; Adler, D. L.; Shapley, J. R.; Nuzzo, R. G. *J. Am. Chem. Soc.* **1997**, 119, 7760.
- (13) Hable, C. T.; Wrighton, M. S. *Langmuir* **1993**, 9, 3284.
- (14) Spendelow, J. S.; Wieckowski, A. *Phys. Chem. Chem. Phys.* **2004**, 6, 5094.
- (15) Wasmus, S.; Vielstich, W. *J. Appl. Electrochem.* **1993**, 23, 120.
- (16) Markovic, N. M.; Gasteiger, H. A.; Ross, P. N.; Jiang, X.; Villegas, I.; Weaver, M. J. *Electrochim. Acta* **1995**, 40, 91.
- (17) Liu, R.; Iddir, H.; Fan, Q.; Hou, G.; Bo, A.; Ley, K. L.; Smotkin, E. S.; Sung, Y. E.; Kim, H.; Thomas, S.; Wieckowski, A. *J. Phys. Chem. B* **2000**, 104, 3518.
- (18) Steigerwalt, E. S.; Deluga, G. A.; Cliffl, D. E.; Lukehart, C. M. *J. Phys. Chem. B* **2001**, 105, 8097.
- (19) Wan, L.-J.; Moriyama, T.; Ito, M.; Uchida, H.; Watanabe, M. *Chem. Commun.* **2002**, 58.
- (20) Lou, Y.; Maye, M. M.; Han, L.; Luo, J.; Zhong, C.-J. *Chem. Commun.* **2001**, 473.
- (21) Liu, P.; Logadottir, A.; Nørskov, J. K. *Electrochim. Acta* **2003**, 48, 3731.
- (22) Steigerwalt, E. S.; Deluga, G. A.; Lukehart, C. M. *J. Phys. Chem. B* **2002**, 106, 760.
- (23) Igarashi, H.; Fujino, T.; Zhu, Y.; Uchida, H.; Watanabe, M. *Phys. Chem. Chem. Phys.* **2001**, 3, 306.
- (24) Massong, H.; Wang, H.; Samjesk, G.; Baltruschat, H. *Electrochim. Acta* **2001**, 46, 701.
- (25) Watanabe, M.; Zhu, Y.; Uchida, H. *J. Phys. Chem. B* **2000**, 104, 1762.
- (26) Iwasita, T.; Hoster, H.; John-Anacker, A.; Lin, W. F.; Vielstich, W.
- (27) Ren, X.; Wilson, M. S.; Gottesfeld, S. *J. Electrochem. Soc.* **1996**, 143, L12.
- (28) Liu, S.-H.; Yu, W.-Y.; Chen, C.-H.; Lo, A.-Y.; Hwang, B.-J.; Chien, S.-H.; Liu, S.-B. *Chem. Mater.* **2008**, 20, 1622.
- (29) Iwasita, T.; Hoster, H.; John-Anacker, A.; Lin, W. F.; Vielstich, W. *Langmuir* **2000**, 16, 522.
- (30) Alayoglu, S.; Nilekar, A. U.; Mavrikakis, M.; Eichhorn, B. *Nat. Mater.* **2008**, 7, 333.
- (31) Nitani, H.; Nakagawa, T.; Daimon, H.; Kurobe, Y.; Ono, T.; Honda, Y.; Koizumi, A.; Seino, S.; Yamamoto, T. A. *Appl. Catal. A: Gen* **2007**, 326, 194.
- (32) Wang, K.; Gasteiger, H. A.; Markovic, N. M.; Ross, P. N. *Electrochim. Acta* **1996**, 41, 2587.
- (33) Watanabe, M.; Uchida, M.; Motoo, S. *J. Electroanal. Chem.* **1987**, 229, 395.
- (34) Deivaraj, T. C.; Lee, J. Y. *J. Power Sources* **2005**, 142, 43.
- (35) Fujiwara, N.; Yasuda, K.; Ioroi, T.; Siroma, Z.; Miyazaki, Y. *Electrochim. Acta* **2002**, 47, 4079.
- (36) Bock, C.; Paquet, C.; Couillard, M.; Botton, G. A.; MacDougall, B. R. *J. Am. Chem. Soc.* **2004**, 126, 8028.

some of the methods used for preparing supported multicomponent Pt-based nanoparticles in general and PtRu in particular. For the latter purpose, Pt and Ru salts (chlorides, nitrates, hydroxides, molecular carbonyl clusters, and acetylacetonates) were reduced in both aqueous and nonaqueous media with H_2 ,^{37,38} N_2H_4 ,³⁹ NaBH_4 ,^{11,34,35,40} $\text{N}(\text{Oct})_4[\text{BEt}_3\text{H}]$,⁴¹ $\text{Al}(\text{Me})_3$,⁴² alcohol,^{30,31,34,36} formaldehyde,⁴³ and formic acid.¹⁵ A major obstacle in obtaining alloy PtRu nanoparticles in solutions is the difference in the reduction rates of the two metals, which favors the formation of either phase-separated entities or of core-shell structures in which one element is totally obscured.⁴⁴ This is an undesirable outcome as the effective oxidation of methanol or CO-contaminated H_2 requires the presence of adjacent Pt and Ru atoms on the surface of the catalyst.^{6,9,45–47} Consequently, a postprecipitation step involving conditioning at high temperatures is usually necessary to obtain well alloyed particles. Since the heat treatment usually causes the aggregation of the catalyst, the direct precipitation of dispersed alloyed PtRu nanoparticles remains a very attractive concept.

While other protocols are available for the coprecipitation of platinum and ruthenium, the reduction in polyols has several important advantages. First, these compounds can act simultaneously as solvents and reducing agents, which results in simpler precipitation systems. Second, the high temperatures at which the “polyol process” is conducted (up to 234 °C)⁴⁸ favor the interdiffusion of the two metals and the formation of alloyed particles. In this article we explore various strategies for developing a polyol process capable of generating well-dispersed alloyed PtRu nanoparticles deposited on carbon supports. While previously ethylene glycol was preferably used in the preparation of both simple and composite metallic particles,^{3,31,36,49,50} this work reveals that propylene glycol (PG) offers better conditions for tailoring the internal composition of PtRu bimetallic nanoparticles. We show that in this polyol it is possible to prepare PtRu nanoparticles in which the distribution

of the two elements from the periphery to the core can be controlled.

Experimental section

A. Materials and Equipment. The aqueous solutions of hexachloroplatinic acid (H_2PtCl_6 , 25.1% Pt) and ruthenium chloride (RuCl_3 , 18.3% Ru) as well as the carbon support (Vulcan XC 72R) were obtained from Umicore (South Plainfield, NJ). All five polyols evaluated were purchased from Alfa Aesar while the Arabic gum was obtained from Flutarom (Carlstadt, NJ). Concentrated solutions of NaOH and HCl were used for pH adjustments. All experiments were carried out in a four-neck 1000 cm^3 spherical glass flask provided with an electrical heating mantle and a power-controlling device. The reaction mixture was stirred using a 72 mm Teflon blade attached through the central neck to a variable speed motor. A condenser, a graduated funnel, and a thermometer were fitted in the remaining necks of the reaction flask.

B. Procedures. *1. Reduction of Individual Metals in Various Polyols.* An amount of precursor solution containing 0.5 g of metal (1.99 g H_2PtCl_6 or 2.73 g RuCl_3) was added to 500 cm^3 of polyol in the reaction vessel. After stirring the solution for 5 min at 300 rpm, the temperature was increased to the boiling point of the polyol at a rate of ~ 3 °C/min while observing the changes in the properties of the reaction mixture (color, turbidity, etc.) and the formation of metal particles.

2. Preparation of Carbon Supported PtRu Nanoparticles. *a. Reductions of Premixed Pt and Ru Salts.* A total of 18.3 g of H_2PtCl_6 solution and 13.1 g of RuCl_3 solution (corresponding to 4.6 g of Pt and 2.4 g of Ru, respectively, or a 1:1 atomic ratio) were added to 550 cm^3 of polyol followed by 1.75 g of Arabic gum previously dissolved in 10 cm^3 of water. The pH was adjusted with a NaOH solution (50% w/v) as specified in Table 2. Next, 7.0 g of carbon powder were added slowly into the polyol solution. After 30 min of stirring, the content of the flask was heated at a rate of 3 °C/min to 170 °C where it was maintained for 10 min before the heating was stopped. The water and volatile byproducts were distilled off during the heating process. When the temperature decreased to ~ 150 °C, 275 cm^3 of cold deionized (DI) water were slowly added to bring the temperature to ~ 100 °C, and the pH was adjusted to ~ 0.7 with concentrated HCl solution. After two hours of stirring at 100 ± 3 °C, the dispersion was cooled at room temperature and the solids were filtered and washed repeatedly with water until the pH of the filtrate was neutral. The mother liquor and the catalyst were collected for analysis and characterization.

b. Sequential Addition of Metal Precursors. In this case, the RuCl_3 solution (corresponding to 2.4 g of Ru) was introduced first into 550 cm^3 of polyol at room temperature. The amounts

- (37) Martins, R. L.; Baldanza, M. A. S.; Schmal, M. J. *Phys. Chem. B* **2001**, *105*, 10303.
- (38) Radmilovic, V.; Gasteiger, H. A.; Ross, P. N. *J. Catal.* **1995**, *154*, 98.
- (39) Aramata, A.; Kodera, T.; Masuda, M. J. *Appl. Electrochem.* **1988**, *18*, 577.
- (40) Shimazaki, Y.; Kobayashi, Y.; Yamada, S.; Miwa, T.; Konno, M. *J. Colloid Interface Sci.* **2005**, *292*, 122.
- (41) Vogel, W.; Britz, P.; Bonnemmann, H.; Rothe, J.; Hormes, J. J. *Phys. Chem. B* **1997**, *101*, 11029.
- (42) Paulus, U. A.; Endruschat, U.; Feldmeyer, G. J.; Schmidt, T. J.; Bönnemann, H.; Behm, R. J. *J. Catal.* **2000**, *195*, 383.
- (43) Liu, Z.; Lee, J. Y.; Han, M.; Chen, W.; Gan, L. M. *J. Mater. Chem.* **2002**, *12*, 2453.
- (44) Yan, X.; Liu, H.; Liew, K. Y. *J. Mater. Chem.* **2001**, *11*, 3387.
- (45) Gasteiger, H. A.; Markovic, N.; Ross, P. N.; Cairns, E. J. *J. Phys. Chem.* **1993**, *97*, 12020.
- (46) Maillard, F.; Lu, G. Q.; Wieckowski, A.; Stimming, U. *J. Phys. Chem. B* **2005**, *109*, 16230.
- (47) Aricò, A. S.; Shukla, A. K.; Kim, H.; Park, S.; Min, M.; Antonucci, V. *Appl. Surf. Sci.* **2001**, *172*, 33.
- (48) Goia, C.; Matijevic, E.; Goia, D. V. *J. Mater. Res.* **2005**, *20*, 1507.
- (49) Larcher, D.; Patrice, R. *J. Solid State Chem.* **2000**, *154*, 405.
- (50) Viau, G.; Brayner, R.; Poul, L.; Chakroune, N.; Lacaze, E.; Fievet-Vincent, F.; Fievet, F. *Chem. Mater.* **2003**, *15*, 486.

Table 1. Formula and Physical Properties of the Polyols Used in This Study

polyol	structural formula	molecular weight	bp, °C
ethylene glycol (EG)	$\text{HO}-\text{CH}_2-\text{CH}_2-\text{OH}$	62.07	198
1,2-propanediol (PG) ^a	$\text{HO}-\text{CH}_2-\text{CH}(\text{OH})-\text{CH}_3$	76.1	189
1,3-propanediol (TMG) ^b	$\text{HO}-\text{CH}_2-\text{CH}_2-\text{CH}_2-\text{OH}$	76.1	214
glycerol	$\text{HO}-\text{CH}_2-\text{CH}(\text{OH})-\text{CH}_2-\text{OH}$	92.1	290
diethylene glycol (DEG)	$\text{HO}-\text{CH}_2-\text{CH}_2-\text{O}-\text{CH}_2-\text{CH}_2-\text{OH}$	106.1	245

^a Propylene glycol. ^b Trimethylene glycol.

Table 2. Summary of the Reaction Conditions and Characteristics of the Samples of Carbon-Supported PtRu Particles Prepared by Heating Polyols Containing both H_2PtCl_6 and RuCl_3

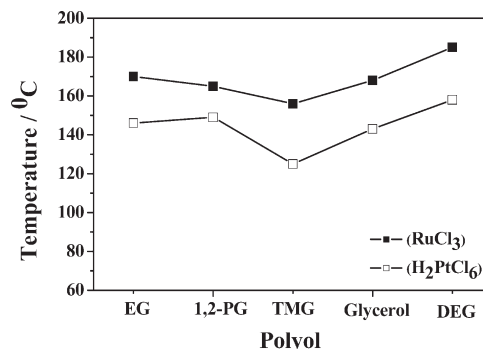
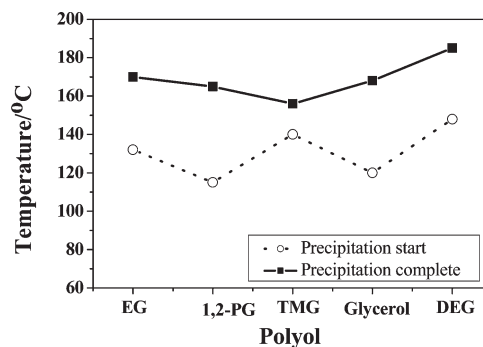
sample	polyol	pH	yield (%)		crystallite size, nm (XRD)	lattice const., Å
			Pt	Ru		
1	PG	3.5	100	>99.0	10.3	3.898
2	PG	5.5	100	>99.0	5.4	3.903
3	PG	9.5	100	>99.0	3.8	3.923
4	DEG	5.5	100	70	3.6	3.927
5	TMG	5.5	100	87	3.4	3.914

and addition sequence of dispersant and carbon supports were the same as in B.2.a. The RuCl_3/C dispersion was next heated to the reaction temperature where 100 cm^3 of the same polyol containing 4.6 g of Pt (as H_2PtCl_6) was added over 30 min from a dropping funnel. The temperature was then increased to $170\text{ }^\circ\text{C}$ where it was maintained for 30 min. The final solids were purified and separated as described in B.2.a.

C. Characterizations. The size of PtRu nanoparticles and their distribution on the carbon support were investigated by TEM (Jeol JEM-1200EX) and FE-SEM (Jeol JSM-7400F). Their crystalline structure was assessed by XRD analysis using a Bruker D8 analyzer. The X-ray photoelectron spectrometry measurements were carried out using Mg $\text{K}\alpha$ radiation. A Leybold LH11A electron energy analyzer was operated at a pass energy of 72 eV. Shirley-type background subtraction⁵¹ and relative sensitivity correction factors were applied to the whole Pt 4f doublet region and the Ru $3p_{3/2}$ signal after Gaussian/Lorentzian line shape analysis. The correction factors used were 3.9 for Pt 4f and 1.92 for Ru $3p_{3/2}$. The Ru 3p region was considered because of the partial overlap between the Ru $3d_{3/2}$ signal and the C 1s region of the carbon support. The catalysts were supported as loose powders on a gold-coated tantalum support, and the analyses were performed at pressures below 6×10^{-8} mbar using a $4\text{ mm} \times 7\text{ mm}$ aperture. The standard was run before and after the analysis of each catalyst sample. The surface composition of the catalyst was estimated by the ratio between the surface concentrations of the two metals determined from the Ru $3p_{3/2}$ and Pt 4f signals. The concentration of unreduced Pt and Ru in the liquid phase was determined by ICAP analysis (Thermo Jarrell Ash 61E Trace Analyzer).

Results and Discussion

The key in the precipitation of true alloy PtRu nanoparticles is to provide similar reduction rates for the two metals. As indicated by the values of the redox potentials in aqueous solutions, the Ru(III) species are in general more difficult to reduce than Pt(IV). In polyols the situation is likely more complicated because the oxidation of polyalcohols can take place via different paths depending on the relative location of the hydroxyl groups and reaction conditions.^{36,49,52–54} To compare the reduction of the two elements in this case, their salts were reduced separately following the protocol described in section B.1 in the polyols listed in Table 1. Figure 1 presents the

**Figure 1.** Temperatures ($\pm 3\text{ }^\circ\text{C}$) of particle formation for the reduction of H_2PtCl_6 and RuCl_3 in various polyols.**Figure 2.** Temperature ranges for the reduction of RuCl_3 in different polyols.

temperature at which the metallic salts are completely reduced in each solvent (i.e., the concentration in the liquid phase measured by ICAP is below 1 ppm). The data show that Ru(III) species are reduced at consistently higher temperature than Pt(IV), as predicted by the values of the redox potentials for aqueous solutions. In contrast with the reductions in monohydroxylic alcohols, the reduction temperature was not a simple function of the molecular weight or boiling point of the polyol. For example, despite having a lower molecular weight than 1,3-propanediol (TMG), ethylene glycol reduced both metals at a higher temperature. Furthermore, in TMG the metals were reduced at a lower temperature than in PG, although its boiling point is significantly higher ($214\text{ }^\circ\text{C}$ vs $189\text{ }^\circ\text{C}$). Structural features, such as the relative position of the hydroxyl groups, played also an important role as illustrated by the difference between the two propanediols. The investigations also revealed a significant difference between the kinetics of the reduction of the two metals. In all polyols, the Pt(IV) species were reduced rapidly and completely in a narrow range of temperature ($2\text{--}3\text{ }^\circ\text{C}$). In contrast, likely because of the multistage reduction of Ru(III) to Ru(0),⁵⁰ the reaction in the case of ruthenium was much slower and occurred over a broad temperature range, which depended on the solvent used (Figure 2).

Because it provided the smaller reduction temperature gap (Figure 1), PG was considered to be the best option for obtaining PtRu alloyed nanoparticles and was thus used in the rest of the experiments. The next focus of the investigations was to find if the difference in the reactivity

(51) Shirley, D. A. *Phys. Rev. B* **1972**, 5, 4709.

(52) Bock, C.; MacDougall, B.; LePage, Y. *J. Electrochem. Soc.* **2004**, 151, A1269.

(53) Shono, T.; Matsumura, Y.; Hashimoto, T.; Hibino, K.; Hamaguchi, H.; T. A. *J. Am. Chem. Soc.* **1975**, 97, 2546.

(54) Schaefer, H. J.; R., S. *Tetrahedron* **1991**, 47, 715.

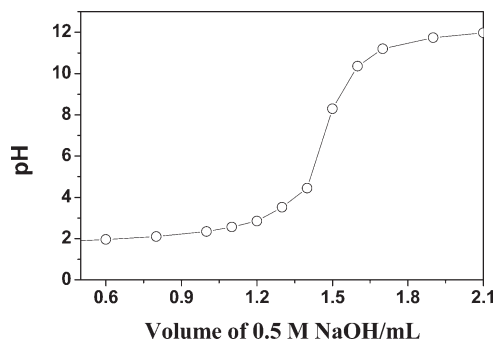


Figure 3. Titration of a RuCl_3/PG solution (1000 ppm) with 0.5 M NaOH at room temperature.

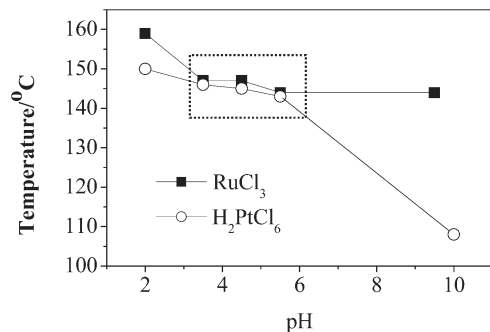


Figure 4. Variation of the reduction temperature of RuCl_3 (■) and H_2PtCl_6 (○) in PG with pH.

of platinum and ruthenium species can be further minimized by varying the pH of the polyol solutions. For this purpose, the normally acidic solutions of H_2PtCl_6 and RuCl_3 were titrated with concentrated NaOH in both water and PG. The addition of the base to the RuCl_3 aqueous solution caused the hydrolysis of the Ru(III) species and the formation of a brownish-black precipitate at pH values above ~ 3.0 . In PG, regardless whether RuCl_3 was titrated alone (Figure 3) or in the presence of H_2PtCl_6 , the precipitation was not observed even at pH values as high as 12.0. In contrast, the titration of H_2PtCl_6 in both solvents resulted in clear solutions and titration curves similar to the one showed in Figure 3.

When solutions of individual metal precursors adjusted at different pH values in the range from 2.0 to 12.0 were heated in PG, the temperature at which the metals were fully reduced decreased gradually (Figure 4). In the pH range from 3.0 to 6.0, however, the values of the reduction temperatures for Pt(IV) and Ru(III) were similar. This behavior is caused by the difference in the stability of the two species vis-à-vis hydrolysis. Since the substitution of Cl^- with OH^- in the $[\text{PtCl}_6]^{2-}$ complex is negligible in the conditions explored, the decrease in the reduction temperature for Pt reflects mainly the gradual increase in the reducing ability of the polyol with pH. In the case of ruthenium, the addition of base easily destabilizes the weaker ruthenium chloro complex but the hydrolysis of Ru(III) species in polyol does not occur at neutral pH (see Figure 3). As a result, in the pH range from 3.0 to 6.0 more labile and thus more easily reduced Ru(III) species are formed. At pH 10.0, however, the Ru(III) ions are completely hydrolyzed yielding more stable species.

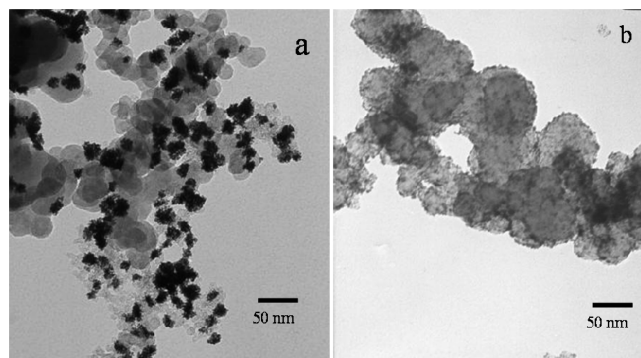


Figure 5. Typical TEM images of carbon-supported PtRu catalysts prepared in PG at pH = 3.5 (a) and 9.5 (b).

As a result, the reduction temperature remains high despite the increased reducing power of PG.

The above findings suggest that alloyed PtRu particles may form in this pH window by simply heating solutions containing both H_2PtCl_6 and RuCl_3 . To verify this assumption, carbon-supported PtRu particles were prepared at different pH values following the protocol described in Section B.2.a. The catalyst composition selected was 50% C/50% metal by weight (Pt:Ru atomic ratio 1:1), as this composition has been the most extensively investigated^{29,45} and has been found to give the best performance for the oxidation of CO-contaminated hydrogen. The pH values selected (listed in Table 2) were 3.5, 5.5, and 9.5 for PG and 5.5 for two other polyols (TMG and DEG). The pH 3.5 and 5.5 represent the approximate boundaries of the range identified in Figure 4 (boxed area), while the value of 9.5 was chosen to verify if the lower reduction temperature observed for Pt at high pH in the previous set of experiments results in faster nucleation and the formation of smaller metallic particles. (Note: During the reduction process, the pH of the dispersion decreases slightly as a result of the protons released from the oxidation of the polyol). The TEM (Figure 5) and XRD studies showed that the size of the PtRu nanoparticles decreased and their dispersion on the support improved with the increase in the pH. This result is in agreement with the findings of Ying et al. who also reported a decrease in particle size with the increase in pH.⁵⁵ At pH 5.5, the particles obtained in TMG and DEG were smaller (Table 2) and slightly more uniform than those obtained in PG (Figures 5 and 6). However, since the reduction yield for Ru was low in both DEG and TMG (samples 4 and 5, Table 2) these polyols were not further considered. The effect of pH on the particle size in the polyol process is not well understood. Bock et al.³⁶ suggested that the reduction in size is caused by the stabilizing effect of the glycolate anions formed as a result of the reaction between OH^- ions and the oxidation product of ethylene glycol. It is likely, however, that the increasing reducing strength at higher pH values provides a faster nucleation and thus smaller particles.

The degree of PtRu alloying for the samples summarized in Table 2 was estimated based on the contraction of

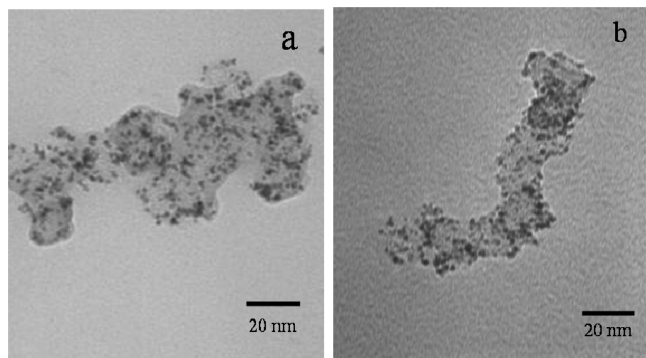


Figure 6. TEM images of PtRu particles prepared in DEG (a) and TMG (b).

the lattice parameter determined from the shift in the position of the XRD peaks. For the PtRu alloy (1:1 atomic ratio), the values of 3.863 Å for bulk⁵⁶ and respectively 3.884 Å³⁸ and 3.886 Å³⁶ for carbon supported nanoparticles have been reported. The higher lattice constant values measured for all experiments listed in Table 2 indicated only a minimal interatomic mixing of the two metals, suggesting that the reduction rates for Pt(IV) and Ru(III) species still differed. This assumption was confirmed visually in an experiment carried out in the absence of the carbon support at pH 5.5. Indeed, the characteristic blue color of the unreduced ruthenium species persisted long after all platinum was reduced, and the lattice constant (3.897 Å) indicated the same low level of interelemental mixing. The clearly observed reduction sequence suggested that a ruthenium-rich surface was formed due to the late reduction of Ru(III) species.⁴¹

Subsequent attempts to minimize the gap between the reduction rates of Pt(IV) and Ru(III) involved the mixing of the two metallic salts at high temperatures. They were based on the observation that, in PG, platinum is rapidly reduced while the reduction of ruthenium takes place at a higher temperature and over a wide range (30–40 °C). Thus, the addition of Pt(IV) ions into the Ru(III)/polyol mixture at a given temperature in this range may trigger the simultaneous reduction of the two metals. Furthermore, since the amount of reduced ruthenium varies with temperature, particles with different surface composition (from Ru rich to Pt rich) may be eventually prepared by increasing the temperature at which the Pt(IV) species are introduced into the system. This was a worthy goal as some studies have shown that an optimum PtRu ratio in the surface provides a higher catalytic activity and an improved catalyst stability.⁴⁷

To verify these assumptions, several samples of carbon-supported PtRu catalysts were prepared by adding a cold polyol solution of PtCl_6^{2-} into Ru(III)/PG solutions maintained at 135 °C, 150 °C, and respectively 165 °C and adjusted at either pH 3.5 or 5.5 (Table 3). The three temperatures selected were at the lower limit, center, and upper limit of the reduction range of Ru(III) in propylene

Table 3. Samples of Carbon-Supported PtRu Catalysts Prepared in PG by Adding the H_2PtCl_6 /Polyol Solution in the RuCl_3 /Catalyst Dispersion at Different Temperatures

sample	~pH	temperature, °C	crystallite size, nm (XRD)	lattice constant, Å
6	3.5	135	3.2	3.852
7	3.5	150	1.7	3.818
8	3.5	165	3.1	3.849
9	5.5	135	2.5	3.864
10	5.5	150	2.3	3.824
11	5.5	165	3.5	3.882

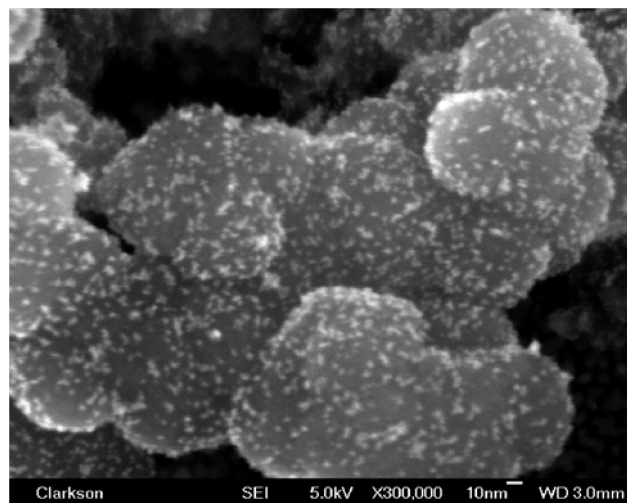


Figure 7. FE-SEM image of carbon-supported PtRu nanoparticles obtained at pH 5.5 and 150 °C (sample 10, Table 3).

Table 4. Quantitative Contribution of Pt and Ru Elements in the Carbon Supported PtRu Catalysts at 135 °C, 150 °C, and 165 °C, Respectively

	sample 6	sample 7	sample 8
Ru 3p _{3/2}	3.44	2.54	2.60
Pt 4f	3.10	2.48	2.81
Ru/Pt surface ratio	1.11	1.02	0.925

glycol (Figure 2), while the two pH values tested were within the optimum range identified in Figure 4. All experiments listed in Table 3 yielded uniform and highly dispersed PtRu nanoparticles, as testified by the FESEM micrograph (Figure 7) of the catalyst obtained at pH 5.5 and 150 °C (sample 10, Table 3). The crystallite size measured by XRD was larger at the extremities of the temperature range than at the center. A similar trend was observed for the lattice parameter, which reached a minimum at 150 °C. The lattice constants of 3.818 Å (pH 3.5) and respectively 3.824 Å (pH 5.5) measured at this temperature were the lowest reported yet and very close to the value for PtRu particles predicted from Vegard's law for a perfect degree of alloying for the fcc model ($a_{\text{PtRu}} = 3.80$ Å).¹²

Despite the similar values of the lattice parameter at 135 and 165 °C (3.852 and 3.848 Å at pH 3.5), the XPS data indicated that the internal structure of the particles obtained in the explored temperature range was quite different, as confirmed by the Ru/Pt ratios calculated from the surface concentrations (Table 4). When H_2PtCl_6 was added at the lower temperature, the particles had a Ru-rich surface, as most Pt(IV) ions were reduced rapidly

(56) Gasteiger, H. A.; Ross, P. N.Jr.; Cairns, E. J. *Surf. Sci.* **1993**, 293, 67.

and completely while the Ru(III) ions were reduced only later, when the temperature was increased to 170 °C. In contrast, at 165 °C particles with a Pt-rich shell were formed as most of the Ru(III) ions were reduced before the H_2PtCl_6 was added into the system. In the middle of the temperature range the two metals were reduced at comparable rates forming a uniform mixed lattice, as indicated by the smaller lattice parameter. Despite the difference in crystallite size, the values of the Ru/Pt ratios reported in Table 4 reflect predominantly the surface composition of the catalyst as the contributions of bulk states decrease with depth.⁵⁷

The role of stabilizing agents in the precipitation of dispersed metallic particles is crucial, especially at high ionic strengths and in nonaqueous solvents. In the case of the synthesis of supported metallic catalysts, these additives also affect the wetting and dispersion of the substrate. Unfortunately, most stabilizers tend to attach rather strongly to metallic surfaces with a detrimental effect on the catalytic activity. For this reason, their complete removal is critical. While postprecipitation oxidative heat treatment is an effective way to eliminate the residual organic matter, it is not suitable for PtRu nanoparticles as the two metals separate at temperatures as low as 220 °C.^{36,52} For this reason, the selection of the dispersing agent in the precipitation of PtRu particles is a challenging task. While several dispersants were tested [poly(ethylene glycol)s with M_w of 200, 1800, and 6000, poly(ethylene imines)], Arabic gum proved to be the most effective dispersant in the studied system. It not only allowed the preparation of small, well dispersed, and

uniform PtRu nanoparticles (Figure 7) but also provided an improved dispersion of the carbon substrate in the polyol. For these reasons, this polymer was added in all precipitation experiments involving the preparation of supported PtRu catalysts. The Arabic gum can be decomposed by chemical hydrolysis at $\text{pH} < 1.0$ and ~ 100 °C leaving a clean metallic surface after washing.

Conclusions

We have explored several practical strategies for synthesizing carbon supported PtRu nanoparticles in polyols. A process that is capable of producing highly dispersed, small, alloyed PtRu particles on carbon support has been developed. Among the polyols explored, propylene glycol was the most suitable for reducing Ru(III) and Pt(IV) ions at relatively low temperatures while providing an environmentally friendly, easily scalable, and cost-effective preparative route. Despite the dissimilar redox potentials of the two species, we have identified reaction conditions and developed processing schemes which allow the two species to form alloyed particles with controlled internal and surface compositions. The codeposition schemes reported provide viable ways to control the degree of mixing in other multicomponent metallic systems and offer a promising direction for future research.

Acknowledgment. This work was funded by a generous grant from Umicore (Hanau/Germany). The authors also thank Dr. Peter Albers (AQura GmbH, Hanau, Germany) for his valuable input in the interpretation of XPS data.

(57) Briggs, D.; Seah, M. P. Wiley & Sons: Chichester, 1990; p 207.